THE ASTROPHYSICAL JOURNAL, 490:L5–L8, 1997 November 20

A DEEP SUBMILLIMETER SURVEY OF LENSING CLUSTERS: A NEW WINDOW ON GALAXY FORMATION AND EVOLUTION

IAN SMAIL,[1,2] R. J. IVISON, [2,3] AND A. W. BLAIN[4]

Received 1997 August 1; accepted 1997 September 23; published 1997 October 24

ABSTRACT

We present the first results of a submillimeter survey of distant clusters using the new Submillimeter Common-User Bolometer Array (SCUBA) on the James Clerk Maxwell Telescope. We have mapped fields in two massive, concentrated clusters, A370 at $z = 0.37$ and Cl 2244−02 at $z = 0.33$, at wavelengths of 450 and 850 μm. The resulting continuum maps cover a total area of about 10 arcmin^2 to 1 σ noise levels less than 14 and 2 mJy beam^{-1} at the two wavelengths, 2–3 orders of magnitude deeper than was previously possible. We have concentrated on lensing clusters to exploit the amplification of *all* background sources by the cluster, improving the sensitivity by a factor of 1.3–2 as compared with a blank-field survey. A cumulative source surface density of $(2.4 \pm 1.0) \times 10^3$ deg^{-2} is found to a 50% completeness limit of ~4 mJy at 850 μm. The submillimeter spectral properties of these sources indicate that the majority lie at high redshift, $z > 1$. Without correcting for lens amplification, our observations limit the blank-field counts at this depth. The surface density is 3 orders of magnitude greater than the expectation of a nonevolving model using the local *IRAS* 60 μm luminosity function. The observed source counts thus require a substantial increase in the number density of strongly star-forming galaxies in the high-redshift universe and suggest that optical surveys may have substantially underestimated the star formation density in the distant universe. Deeper submillimeter surveys with SCUBA should detect large numbers of star-forming galaxies at high redshift and so provide strong constraints on the formation of normal galaxies.

Subject headings: cosmology: observations — early universe — galaxies: evolution — galaxies: formation — gravitational lensing — radio continuum: galaxies

1. INTRODUCTION

Surveys of the local universe have shown that a third of the total bolometric luminosity is emitted at submillimeter and far-infrared wavelengths as a result of reprocessing of starlight by dust (Soifer & Neugebauer 1991). Moreover, some of the most vigorous star-forming galaxies in the local universe are also those in which the effects of dust obscuration are most significant. While there have been striking advances in the identification of "normal" galaxies at high redshift ($z \sim 2$–4) using Lyman dropout techniques (Steidel et al. 1996), such approaches are insensitive to highly obscured star-forming galaxies at these epochs. The presence of at least modest amounts of dust in distant protogalaxies, especially forming spheroids, is expected given the highly metal-enriched ISM which must be present during their formation (e.g., Mazzei & de Zotti 1996). Thus techniques sensititive to obscured distant galaxies should be used to investigate the formation of these populations in the early universe.

Sensitive submillimeter observations present the first opportunity to detect dusty star-forming galaxies at high redshift. At wavelengths around 100 μm, the bulk of the luminosity of normal, star-forming galaxies is reprocessed starlight from dust, so observations in the submillimeter band can provide robust estimates of both the dust mass and total star formation rate in a galaxy. Furthermore, the negative *K*-correction at wavelengths $\lambda \gtrsim 400$ μm means that submillimeter observations select star-forming galaxies at $z \gtrsim 1$ in an almost distance-independent manner, providing an efficient method for the detection of star-forming galaxies at very large redshifts, $z \lesssim 10$ and hence for studying galaxy evolution (Blain & Longair 1993, 1996, hereafter BL96; Blain 1997; Eales & Edmunds 1997; Franceschini, Andreani, & Danese 1997; Guiderdoni, Hivon, & Bouchet 1997).

Most published submillimeter studies of distant galaxies have targeted atypical galaxies (e.g., radio-loud galaxies; Ivison et al. 1998). We report here the first deep submillimeter survey to probe the nature of normal galaxies at moderate and high redshift, $z \gtrsim 0.5$. In this study we have attempted to maximize the available sample of distant galaxies by concentrating on fields in moderate-redshift clusters. While the dominant spheroidal populations of these clusters are expected to be quiescent in the submillimeter band, the infall of field galaxies associated with the growth of the clusters (Smail et al. 1997) means that these fields may contain overdensities of moderate-redshift star-forming galaxies, as compared with "blank" field surveys.

The main attraction of the clusters observed here, however, is that they are strong gravitational lenses, magnifying any source lying behind them (Blain 1997). Given the expected steep rise in the submillimeter counts (BL96), amplification bias could increase the source counts in these fields by a substantial factor, with a maximum predicted surface density of about 10 sources per SCUBA field down to 1 mJy at 850 μm (Blain 1997). Moreover, by targeting those clusters that contain giant arcs (images of distant field galaxies magnified by factors of 10–20), we can also obtain otherwise unachievable sensitivity ($\lesssim 0.1$ mJy at 850 μm) on the dust properties of a few serendipitously positioned normal galaxies at high redshift. The angular scale of the region where these highly magnified high-redshift galaxies is found are also well-matched to the SCUBA field of view.

In the following sections we give details of the observations

[1] Department of Physics, University of Durham, South Road, Durham DH1 3LE, England, UK.
[2] PPARC Advanced Fellow.
[3] Institute for Astronomy, Department of Physics and Astronomy, University of Edinburgh, Blackford Hill, Edinburgh EH9 3HJ, Scotland, UK.
[4] Cavendish Laboratory, Madingley Road, Cambridge CB3 OHE, England, UK.

TABLE 1
SCUBA Observations of A370 and Cl 2244−02

Target	R.A. (J2000)	Decl. (J2000)	λ (μm)	Exposure Time (ks)	Area (arcmin^2)	Flux Density 1 σ (mJy)
Cl 2244−02	22 47 11.9	−02 05 38	450	23.0	4.00	14.0
			850	23.0	5.40	1.9
A370	02 39 53.0	−01 35 06	450	25.7	4.35	13.3
			850	25.7	5.40	1.8

Note.—Units of right ascension are hours, minutes, and seconds, and units of declination are degrees, arcminutes, and arcseconds.

and their reduction and discuss the results within the framework of current theoretical models of galaxy formation and evolution. We adopt $H_0 = 50$ km s^{-1} Mpc^{-1} and $q_0 = 0.5$.

2. OBSERVATIONS AND REDUCTION

These data were obtained using SCUBA (Cunningham et al. 1994) on the James Clerk Maxwell Telescope (JCMT).[5] SCUBA contains a number of detectors and detector arrays cooled to 0.1 K and covering the atmospheric windows from 350 to 2000 μm. In our survey, we operated the 91 element shortwave (SW) array at 450 μm and the 37 element longwave (LW) array at 850 μm, giving half-power beamwidths of 7.″5 and 14.″7, respectively. Both arrays have a 2.′3 instantaneous field of view, and the design of the optics ensures that, with a suitable jiggle pattern for the secondary mirror, fully sampled maps can be obtained simultaneously at 450 and 850 μm. The multiplexing and high efficiency of the arrays means that SCUBA offers a gain in mapping speed of a factor of about 300 as compared with previous detectors.

The observations employed a 64-point jiggle pattern, fully sampling both arrays over a period of 128 s. The pattern was subdivided so that the target position could be switched between the signal and reference every 32 s: a repeating signal-reference-reference-signal scheme, with 16, 1 s jiggles in each. While jiggling, the secondary was chopped at 6.944 Hz by 60″ in azimuth. The pointing stability was checked every hour, and regular skydips were performed to measure the atmospheric opacity. The rms pointing errors were below 2″, while atmospheric zenith opacities at 450 and 850 μm were very stable during the course of each night, the night-to-night variations being in the range 0.98–2.2 and 0.18–0.37, respectively.

The dedicated SCUBA data reduction software (SURF; Jenness 1997) was used to reduce the observations. The reduction consisted of subtracting the reference from the signal after carefully rejecting spikes and data from noisy bolometers. Six quiet bolometers at the edge of each array were used to compensate for spatially correlated sky emission. This reduced the effective noise-equivalent flux density from 100–350 to 90 mJy Hz$^{-1/2}$ at 850 μm (see Ivison et al. 1998). The resulting maps were flat-fielded, corrected for atmospheric attenuation, and calibrated using nightly beam maps of Uranus. The calibrated maps from each night were coadded and then linearly interpolated onto an astrometric grid using an approximately Nyquist sampling, of 2″ and 4″ pixel^{-1} at 450 and 850 μm, respectively, to produce the maps presented in Figure 1 (Plate L1).

The final on-source integration times are listed in Table 1, along with field positions and sensitivity limits. The beams have moderate error lobes, especially at 450 μm; thus we correct our aperture measurements for flux outside the aperture using the measured values from our calibration sources. Even without including a factor to account for the lensing amplification, the data shown in Figure 1 are the deepest submillimeter maps ever published and illustrate the cosmetically clean and flat maps achievable with SCUBA in long integrations.

3. ANALYSIS AND RESULTS

Source catalogs from our fields were constructed using the Sextractor package (Bertin & Arnouts 1996). The detection algorithm requires that the surface brightness in 4 contiguous pixels exceeds a threshold (chosen as ~1 σ of the sky noise; see Table 2), after subtracting a smooth background signal and convolving the map with a 4 × 4 pixel top-hat filter. The numbers of objects (N) detected in each field are given in Table 2, indicating that our observations are far from being limited by confusion: there are ~60 beams per source.

To assess the contribution of noise to our catalogs we reran the detection algorithm on the negative fluctuations in the map. This gave a simple estimate of the number of false-positive detections that may arise from the noise, assuming that the noise properties of the map are Gaussian. We estimate that there are no false detections in our catalogs (N_{-ve}; see Table 2), so all the detections are real. The presence of the brightest source in the reference beams (60″ to the east and west in the 850 μm map of A370) was disregarded. This detection does confirm, however, the reality of positive features at this faint level, while the absence of any other negative detections limits the number of luminous sources which can lie in the regions covered by the reference beams.

Second, to determine the completeness of our sample we added a faint source to the maps repeatedly, reran our detection algorithm, and estimated the efficiency of detecting this source

[5] The JCMT is operated by the observatories on behalf of the UK Particle Physics and Astronomy Research Council, the Netherlands Organization for Scientific Research, and the Canadian National Research Council.

TABLE 2
Submillimeter Source Counts

Target	λ (μm)	Threshold (mJy beam^{-1})	Min. Area (arcsec^2)	N	N_{-ve}	$S_{80\%}$ (mJy)	$S_{50\%}$ (mJy)
Cl 2244−02	450	16.0	16	0	0	135	63
	850	1.9	64	2	0	5.5	3.9
A370	450	16.0	16	1	0	140	84
	850	1.8	64	4	0	5.4	3.9

as a function of its flux density. This provides a reliable estimate of the visibility of a faint compact source in the maps. The template source was a scaled version of our calibration source, Uranus. The estimated 80% and 50% completeness limits of the catalogs derived from these simulations are listed in Table 2 as $S_{80\%}$ and $S_{50\%}$. The incompleteness limits are relatively bright for the 450 μm maps because a large proportion of the flux density (about 40%) is found in the low surface brightness wings of the beam. The simulations also indicate that the measured 850 μm flux densities are unbiased and are typically accurate to 10% at 25 mJy and 30% at 4 mJy.

We discuss the detailed properties of the sources in another paper, where we also place limits on the dust masses of the numerous strongly lensed distant galaxies covered by our maps. However, we note that, based on their weak or nondetection at 450 μm, all of the 850 μm sources in our sample appear to have the submillimeter spectral characteristics of distant ($z \gtrsim 1$) star-forming galaxies and are thus unlikely to be associated with the clusters.

Converting the observed number of sources into a surface density and correcting for incompleteness, we determine a cumulative number density across our two fields of $(2.4 \pm 1.0) \times 10^3$ deg^{-2} down to a 50% completeness limit of 4 mJy at 850 μm (all errors include only Poisson contributions). At 450 μm, the single source we detect places only a very weak limit on the likely surface density of the order of 1×10^3 deg^{-2} brighter than 80 mJy.

We now estimate the likely lens amplification factors and so place tighter limits on the typical blank-field counts. Because the distances to the detected sources are unknown, this estimate will, by necessity, be crude, and so we have not attempted a detailed analysis. The cluster potentials are modeled as isothermal spheres with masses and centers determined from the redshifts and observed shapes of the giant arc in each cluster (Kneib et al. 1993; Smail et al. 1996). In these models the mean amplification factors for typical background sources ($z \gtrsim 1$) are about 2 and 1.3 in the regions covered by our maps of A370 and Cl 2244−02, respectively, while the observed area of the maps (5.4 arcmin^2 at 850 μm) corresponds to 1.8 and 4.0 arcmin^2 in the respective source planes. Correcting the flux densities of our sources to take account of the probable lens amplifications but not correcting for incompleteness, we predict the source counts presented in Figure 2. These indicate integrated number densities in blank fields of $(2.5 \pm 1.4) \times 10^3$ (similar to the observed value, due to the source counts having a form close to $S^{0.4}$) and $(3.6 \pm 1.6) \times 10^3$ deg^{-2} to flux limits of 4 and 3 mJy, respectively, at 850 μm.

From the flux densities associated with the resolved sources in the fields we calculate lower limits to the background radiation intensities of 2.6 and 2.4×10^{-10} W m^{-2} sr^{-1} at wavelengths of 450 μm and 850 μm, respectively, averaged over both fields. By extrapolating the 850 μm counts using our best-fit model (Fig. 2 and § 4) to faint flux densities, we estimate total intensities of extragalactic background radiation from discrete sources of about 26–28 and 4.4–6.7 $\times 10^{-10}$ W m^{-2} sr^{-1} at wavelengths of 450 and 850 μm, respectively. These background radiation intensities are broadly consistent with the tentative detection of an isotropic component of the background radiation in the submillimeter by Puget et al. (1996), who inferred $\nu I_\nu = (23 \pm 20)$ and $(2.7 \pm 2.0) \times 10^{-10}$ W m^{-2} sr^{-1} at wavelengths of 450 and 850 μm, respectively. If we assume that all of the background radiation intensity we infer is due to the formation of massive stars, then we expect that a density parameter of heavy elements of $\lesssim 6 \times 10^{-4}$ will have accumulated in the universe by the present epoch. This density corresponds to about 1.1% of the density parameter in baryons if $\Omega_b = 0.05$, and so it is fully consistent with present limits. We reiterate, however, that these are tentative estimates, the accuracy of which depends on the models assumed for both the lens and the form of the counts of distant galaxies.

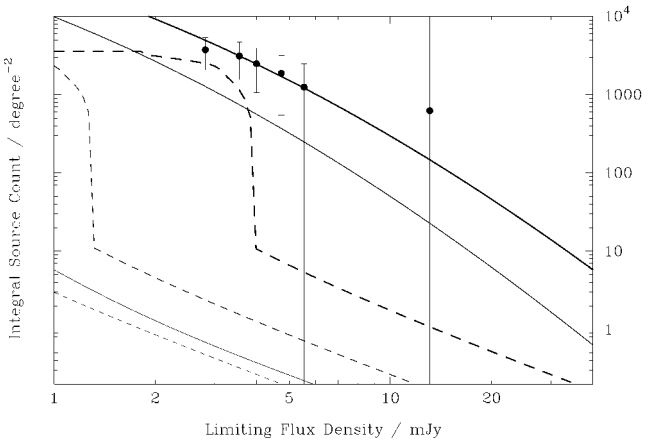

FIG. 2.—Models of the integral number counts of sources at 850 μm in a parametric model of galaxy evolution (BL96) and from a simple model based on the limits on strongly star-forming systems in optical surveys of distant galaxies. The observations are represented by filled circles with Poisson errors; errors are not independent on the various points. The observations have been corrected for the effects of lens amplification using simple lens models, but not corrected for incompleteness. Solid curves represent, in order of increasing predicted counts, models that include: no evolution; $(1 + z)^3$ evolution with $z_{\max} = 2$ and $z_0 = 5$ (model A); and $(1 + z)^3$ evolution with $z_{\max} = 2.6$ and $z_0 = 7$ (model B). Dashed lines represent models where we fill the universe across $z = 0$–10 with a constant density (0.6×10^{-4} Mpc^{-3}) of star-forming galaxies with fixed star formation rates. In order of increasing predicted counts, dashed lines represent star formation rates for the population of $M = 20$, 50, and 150 $M_\odot$ yr^{-1}, where we have assumed a dust temperature of $T = 60$ K. Clearly only models including high densities of strongly star-forming galaxies are compatible with the observed surface density of sources.

4. DISCUSSION

Due to the negative K-corrections expected for distant galaxies, submillimeter observations provide a good estimate of the volume density of luminous star-forming galaxies at $z \gtrsim 1$. In the absence of redshifts for all the sources, the evolution of this population can be understood by comparing parameterized models to the counts (BL96). The BL96 models are based on the 60 μm luminosity function of *IRAS* galaxies (Saunders et al. 1990) and assume that the luminosities evolve as $(1 + z)^3$ out to a redshift, $z_{\max}$, and then maintain the enhanced luminosity out to a cutoff redshift, z_0. The form of this evolution is motivated by the observations of similar behavior in both the radio galaxy and QSO number counts (Dunlop & Peacock 1991) as well as the luminosity density of field galaxies at $z < 1$ (Lilly et al. 1996). BL96 also give predicted counts for a nonevolving model using the same luminosity function. The adopted parameters for the models described in that paper give source counts which roughly span the range predicted by other similar works (e.g. , Guiderdoni, Hivon, & Bouchet 1997). In Figure 2, we plot both the no-evolution case and two other parametric models based on BL96: model A—model 2 in BL96—with values of $z_{\max} = 2$ and $z_0 = 5$; and model B with values of $z_{\max} \simeq 2.6$ and $z_0 = 7$, although most combinations of $z_{\max} \simeq 2.2$–2.9 and $z_0 \gtrsim 5$ give com-

parable results. Model B was used to estimate the total background radiation intensity discussed in § 3.

From Figure 2 it can be seen that the no-evolution predictions fall short by 2–3 orders of magnitude of the observations. Thus, this first analysis of a deep submillimeter survey indicates that the number density of strongly star-forming galaxies, and so the mean star formation rate in the distant universe, is considerably larger than that seen locally. To estimate the extent of this evolution we assume that all the detected sources lie beyond the clusters. We then require strong evolution, of the form given in model B, out to $z > 2$ to fit the 850 μm counts. For consistency, we check the predictions from model B for the observed counts at 450 μm; 0.7 sources are expected in the two fields, in agreement with the single detection.

We conclude from the 850 μm counts that the integrated star formation rate in the universe, as traced by the number density of the most luminous sources, must continue to rise out to beyond $z > 1$ ($z > 2$ in our parametric models), extending the trend observed at $z < 1$ (Lilly et al. 1996). For sources at $z \gtrsim 1$, the typical luminosity we infer is $L_{\rm FIR} \sim (0.5\text{–}1.0) \times 10^{13}\, L_{\odot}$, with a star formation rate of $M \gtrsim (100\text{–}300)\, M_{\odot}\ {\rm yr}^{-1}$. Using the observed surface density of these objects and assuming a constant space density of sources between $z = 1$–5, we would predict a number density of strongly star-forming galaxies of $N(M \gtrsim 150\ M_{\odot} {\rm yr}^{-1}) \sim 1.2 \times 10^{-4}\ {\rm Mpc}^{-3}$, at $z \gtrsim 1$.

Limits on the number density of strongly star-forming galaxies at $z \sim 2$–3.5 have recently been published by Madau et al. (1996, hereafter M96) on the basis of Lyman dropout surveys. Their limit is $N(M > 20\ M_{\odot}\ {\rm yr}^{-1}) < 0.6 \times 10^{-4}\ {\rm Mpc}^{-3}$. We plot in Figure 2 three models using this number density of sources to uniformly populate the volume from $z = 0$–10, but allowing the corresponding star formation rate to vary: $M = 20$, 50, and $150\, M_{\odot}\ {\rm yr}^{-1}$. These values represent that originally given by M96, the M96 limit corrected for dust extinction as suggested by Pettini et al. (1997), and a mean star formation rate closer to that needed to fit our observations. A galaxy population consistent with the limits from M96 predicts a source density 3 orders of magnitude lower than that observed (see Fig. 2). Even if the modest dust extinction proposed by Pettini et al. is included, we still underpredict the observed surface densities (unless the dust in this population is very cold, i.e., $T = 40$ K, with very large dust masses). To match the observed surface density of 850 μm sources we must significantly increase the mean star formation, either by further increasing the star formation rate associated with the optically selected samples (see Meurer et al. 1997) or by introducing a population of strongly star-forming, but highly obscured, distant galaxies missed in these samples. Deeper submillimeter surveys (BL96; Pearson & Rowan-Robinson 1996) are necessary to differentiate between these possibilities and hence provide an unbiased view of star formation in the distant universe.

5. CONCLUSIONS

We have presented the first submillimeter survey of the distant universe, deep enough that we should detect the evolving galaxies predicted by current theoretical models while at the same time covering a sufficiently large area to be statistically reliable. We derive cumulative source counts of $(2.4 \pm 1.0) \times 10^{3}\ {\rm deg}^{-2}$ down to 4 mJy at 850 μm.

The surface density of faint sources in the submillimeter far exceeds a simple nonevolving model using the locally observed 60 μm galaxy luminosity function. Thus our observations require a substantial increase in the number density of strongly star-forming galaxies at $z \gtrsim 1$.

Comparison of our observations with the predictions of simple parametric models implies that the luminosity density of the brightest submillimeter sources continues to increase out to $z > 1$. Models based upon the properties of star-forming galaxies from optically selected samples of distant galaxies (Madau et al. 1996) significantly underestimate the observed surface density of submillimeter sources. We suggest that such samples may be missing a considerable proportion of the star formation in dust-obscured galaxies at high redshift. We conclude that question of the evolution of the star formation density in the distant universe and hence the epoch of galaxy formation is still very much open.

We thank the SCUBA development and commissioning team for providing an efficient and user-friendly instrument, and Ian Robson for his support, enthusiasm, and drive to see the best science done with the JCMT and SCUBA. We wish to thank Richard Bower, Richard Ellis, Carlos Frenk, Wayne Holland, Tim Jenness, Jean-Paul Kneib, and Malcolm Longair for useful conversations and help. We also thank an anonymous referee for comments that clarified the content and presentation of this Letter.

REFERENCES

Bertin, E., & Arnouts, S. 1996, A&A, 117, 393
Blain, A. W. 1997, MNRAS, in press
Blain, A. W., & Longair, M. 1993, MNRAS, 264, 509
———. 1996, MNRAS, 279, 847 (BL96)
Cunningham, C. R., Gear, W. K., Duncan, W. D., Hastings, P. R., & Holland, W. S. 1994, Proc. SPIE, 2198, 638
Dunlop, J. S., & Peacock, J. A. 1991, MNRAS, 247, 19
Eales, S. A., & Edmunds, M. G. 1997, MNRAS, 286, 732
Franceschini, A., Andreani, P., & Danese, L. 1997, MNRAS, submitted
Guiderdoni, B., Hivon, E., & Bouchet, F. R. 1997, astro-ph/9707134
Ivison, R. J., et al. 1998, ApJ, in press
Jenness, T. 1997, Starlink User Note 216.1
Kneib, J.-P., Mellier, Y., Fort, B., & Mathez, G. 1993, A&A, 273, 367
Lilly, S. J., Le Fevre, O., Hammer, F., & Crampton, D. 1996, ApJ, 460, L1
Madau, P., Ferguson, H. C., Dickinson, M. E., Giavalisco, M., Steidel, C. S., & Fruchter, A. 1996, MNRAS, 283, 1388 (M96)
Mazzei, P., & de Zotti, G. 1996, MNRAS, 279, 535
Meurer, G. R., Heckman, T. M., Lehnert, M. D., Leitherer, C., & Lowenthal, J. 1997, AJ, 114, 55
Pearson, C., & Rowan-Robinson, M. 1996, MNRAS, 283, 174
Pettini, M., Steidel, C. C., Dickinson, M. E., Kellogg, M., Giavalisco, M., & Adelberger, K. L. 1997, astro-ph/9707200
Puget, J.-L., Abergel, A., Bernard, J.-P., Boulanger, F., Burton, W. B., Désert, F.-X., & Hartmann, D. 1996, A&A, 308, L5
Saunders, W., Rowan-Robinson, M., Lawrence, A., Efstathiou, G., Kaiser, N., Ellis, R. S., & Frenk, C. S., 1990, MNRAS, 242, 318
Smail, I., Dressler, A., Kneib, J.-P., Ellis, R. S., Couch, W. J., Sharples, R. M., & Oemler, A. 1996, ApJ, 469, 508
Smail, I., Edge, A. C., Ellis, R. S., & Blandford, R. D. 1997, MNRAS, in press
Soifer, B. T., & Neugebauer, G. 1991, AJ, 101, 354
Steidel, C. C., Giavalisco, M., Pettini, M., Dickinson, M., & Adelberger, K. L. 1996, ApJ, 462, L17

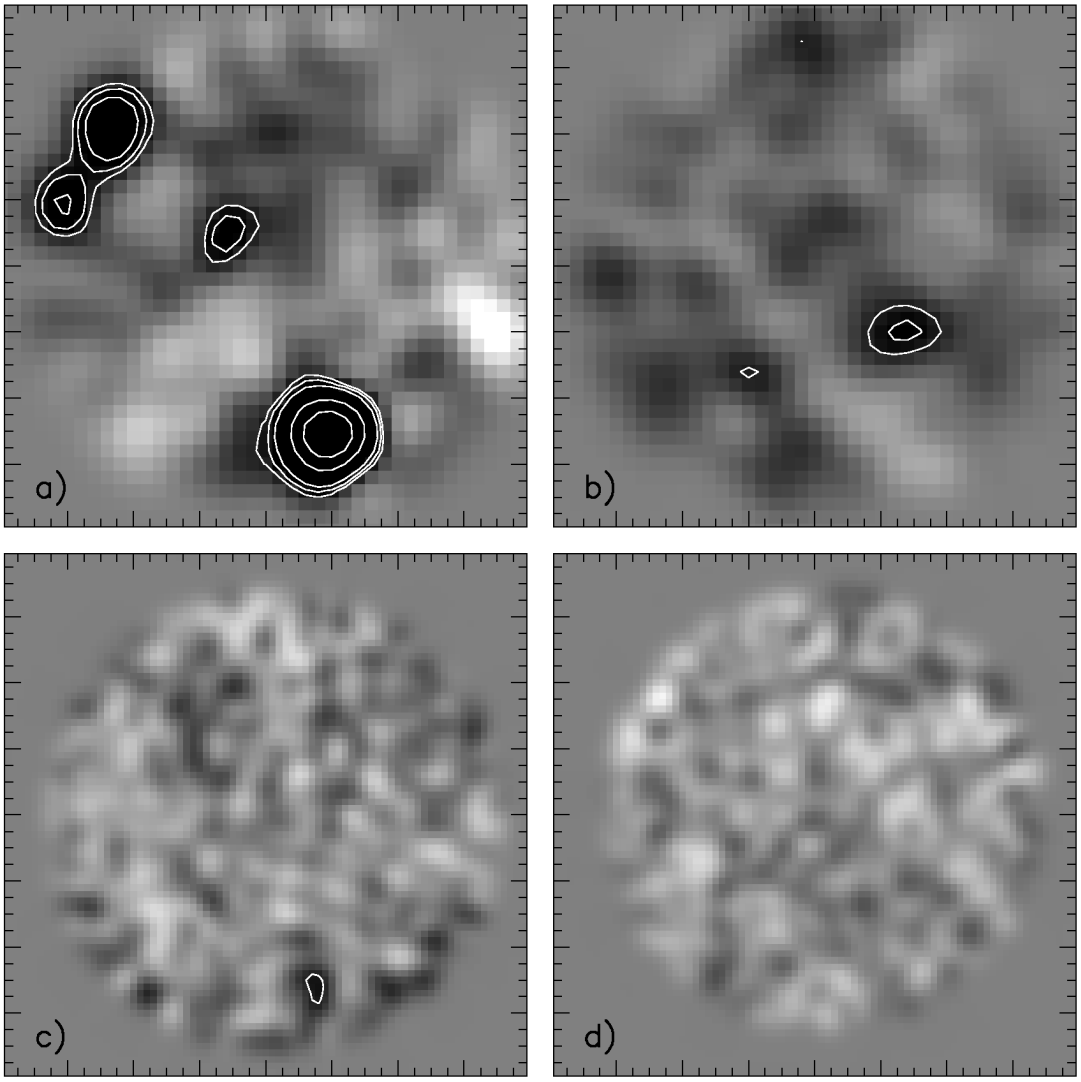

FIG. 1.—450 and 850 μm maps of the two fields: (*a*) A370, 850 μm; (*b*) Cl 2244−02, 850 μm; (*c*) A370, 450 μm; (*d*) Cl 2244−02, 450 μm. The maps are smoothed to the instrumental resolution at each wavelength and have had their boundaries apodized to remove regions on the outskirts with low effective exposure times resulting from the rotation of the field of view during our long exposures. They are displayed as a gray scale from -4 σ to 4 σ; the contours are positive and show 3, 4, 5, 10, and 15 σ for each field. The major tick marks are 20″ in all panels.

SMAIL, IVISON, & BLAIN (see 490, L6)